applied sciences

MDPI

Article

Application of PolyJet 3D Printing in Production of Flexographic Printing Plates

Joanna Izdebska-Podsiadły * and Adam Lasecki

Department of Printing Technology, Institute of Mechanics and Printing, Faculty of Mechanical and Industrial Engineering, Warsaw University of Technology, Konwiktorska 2, 00-217 Warsaw, Poland
* Correspondence: joanna.podsiadly@pw.edu.pl; Tel.: +48-22-234-33-57

Abstract: The aim of this study was to investigate whether PolyJet technology, which uses rubber-like materials for printing and is known for its high resolution and performance, could be suitable for producing flexographic printing plates. In our research, we designed test plates that were printed using PolyJet technology with TangoBlackPlus FLX9870-DM resin. These 3D-printed plates were evaluated for their resistance to various flexographic inks and solvents, and their contact angles were measured. Subsequently, the prints were made on a Flexiproof device using water-based ink with both the test plates and traditional photopolymer plates across six different substrates. The print quality was assessed using densitometry and spectrophotometry. Our findings indicate that the 3D-printed plates are suitable for printing solid areas and lines with water-based inks. However, the print quality of the 3D-printed plates is slightly lower than that of the photopolymer plates, with the optical density values for the high-quality prints on coated papers being approximately 10% lower. Additionally, the plates printed with TangoBlack Plus resin appear to be suitable for UV inks due to their high resistance, but they are not resistant to the solvents used in solvent-based inks.

Keywords: additive manufacturing; 3D printing; PolyJet; flexographic printing; printing plates; prints quality

check for updates

Citation: Izdebska-Podsiadły, J.; Lasecki, A. Application of PolyJet 3D Printing in Production of Flexographic Printing Plates. *Appl. Sci.* **2024**, *14*, 8593. https://doi.org/10.3390/app14198593

Academic Editor: Fuji Wang

Received: 21 August 2024
Revised: 19 September 2024
Accepted: 20 September 2024
Published: 24 September 2024

Copyright: © 2024 by the authors. Licensee MDPI, Basel, Switzerland. This article is an open access article distributed under the terms and conditions of the Creative Commons Attribution (CC BY) license (https://creativecommons.org/licenses/by/4.0/).

1. Introduction

Flexographic printing is currently the only classic printing technology, i.e., using a printing form, that continues to experience rapid development and growth [1,2]. This growth is linked to the expansion of the packaging printing sector [3]. Flexographic printing is particularly popular in many industries due to its ability to print on a variety of printing substrates, such as paper, cardboard, or plastic films, using a flexible printing plate and liquid inks [4,5].

Due to market changes like reduced print runs, personalized products, and shorter promotional runs, traditional printing techniques are being replaced by digital printing [6–8]. Even in flexographic printing, the need for rapid preparation of new printing plates and changing orders on the printing machine is increasing, making it reasonable to consider using additive manufacturing (AM) to produce flexographic plates. Additive manufacturing, also known as 3D printing, is a technology that has been around for some time but continues to advance and find new applications [9,10]. There are various technologies [11–13] and materials [14–16] used in this field, which open up opportunities for new uses of additive manufacturing [17,18]. One potential application is the production of flexographic plates, as these technologies are well-suited for this purpose. It is possible to create parts from materials with properties similar to rubber. In fact, rubber was originally used for the preparation of flexographic plates—but nowadays mainly photopolymers are used [4,19,20]. Moreover, AM technologies that use rubber-like polymeric materials are known for producing highly accurate models.

Polymers, from which flexographic printing plates are commonly made, are the basic material used in AM technologies such as stereolithography (SLA), Digital Light Processing

(DLP), Continuous Liquid Interface Production (CLIP), PolyJet (PJ), Multi-Jet Printing (MJP), Fused Deposition Modeling (FDM), Fused Filament Fabrication (FFF), Direct Ink Writing (DIW), Selective Laser Sintering (SLS), Multi-Jet Fusion (MJF), and Laminated Object Manufacturing (LOM), [11,21,22]. Some of these AM techniques, including SLA, DLP, CLIP, PJ, MJP, DIW, and FDM/FFF, allow for the printing of flexible designs using rubber-like materials [14]. In addition, Vat Photopolymerization (VPP) processes (which include SLA, DLP, and CLIP) and Material Jetting (MJT) processes (which include PJ and MJP) use liquid polymer compositions with a wide range of resins to create models. Flexographic printing plates, due to the deformation that occurs during ink transfer from the printing plate to the printing substrate, are made of flexible materials for precisely this reason [23,24].

Considering printing resolution, the best results can be achieved with the MJT and VPP processes. The resolution for MJT ranges from 10 to 28 µm, while for VPP, it ranges from 10 to 140 µm [11]. In terms of dimensional accuracy and model deformation, MJP and PJ technologies, alongside SLA and MJF, also perform well. For MJT systems, the dimensional accuracy is ±0.1–0.2% with a typical lower limit of ±0.02–0.1 mm. In comparison, the dimensional accuracy for SLA and MJF is ±0.2% with a lower limit of ±0.2 mm [11]. Among the mentioned AM techniques, MJT technologies seem to be the most useful for preparing a flexographic printing plate. They provide the highest accuracy in the produced model and allow us to make a part with a similar hardness and flexibility to a traditional photopolymer plate. PolyJet is a variation of the Material Jetting (MJT) process developed by Objet Geometries. The model is created from photopolymer resin and support material using ink jet print heads and fixed with UV light immediately after application [25–27]. The printed model requires post-processing, which involves the removal of supporting elements by blowing them out with compressed air or washing them out with water at a higher pressure. The undoubted advantages of this technology are the high resolution of the built parts while at the same time maintaining a high speed, the high accuracy and repeatability of the process, the wide spectrum of available materials, the clean and easy method of removing the support material, and the high simplicity of system operation [28–30].

There have been limited studies on the use of AM for the preparation of flexographic printing plates [31–36], with none utilizing the PolyJet technology proposed in our work. Thus, Maksud et al. [31] conducted preliminary research using 3D printing for line reproduction and the formation of micro- and nano-structures when creating a PDMS mold for micro-flexographic printing. Meanwhile, Huange et al. [32] studied the effect of prepolymers and UV-fixed monomers on flexographic plate formation and its performance and printability. He demonstrated the correctness of the ink transfer from the plate to the substrate for an optimally selected prepolymer and monomer composition. Tsakos [33], on the other hand, prepared three different printing plates, two using FDM technology and one using SLA technology. At the same time, not all of the plates had the right flexibility and could be used for printing, and deformation of the letters and logos was observed on the resulting prints, as well as the reflected pattern (grids) of the plate's uneven surface from FDM printing. Zheng et al. [34] also tested and demonstrated the feasibility of using SLA technology to prepare flexographic printing plates and showed that the line width and line edge straightness were comparable to those specified for conventional printing plates on the market. In another study, Zheng [36] examined the factors affecting the process of creating a flexographic printing plate using SLA technology and their impact on quality. Lastly, Hassan et al. [35] explored the effect of printers working with MEX technology and different filaments on the quality of a master mold for micro flexographic printing.

In our study, we explored the feasibility of producing a flexographic plate using PolyJet technology. We also investigated its durability during the printing process and analyzed the impact of the printing substrate and raster cylinder linearity on print quality. Additionally, we compared the results with those obtained from traditionally prepared printing plates. To the authors' knowledge, no previous research has been conducted on this specific topic regarding flexographic plates produced using PolyJet technology.

Furthermore, no extensive studies on the quality of prints produced with plates printed using any 3D-printing technology have been published to date.

2. Materials and Methods

2.1. Preparation of the Printing Forms Design

The design of the test plate for 3D printing was prepared in Autodesk Inventor (Autodesk Inc., San Francisco, CA, USA). The test plate included the following fields: solid printed areas (with 100% coverage, also known as apla) and raster fields with 75%, 50%, and 10% coverage (representing shadows, halftones and bright parts of the reproduced image, respectively) (Figure 1b), as well as microlines with thicknesses from 0.1 mm to 0.35 mm in 0.05 mm increments. The distribution of elements on the test plate is shown in Figure 1a.

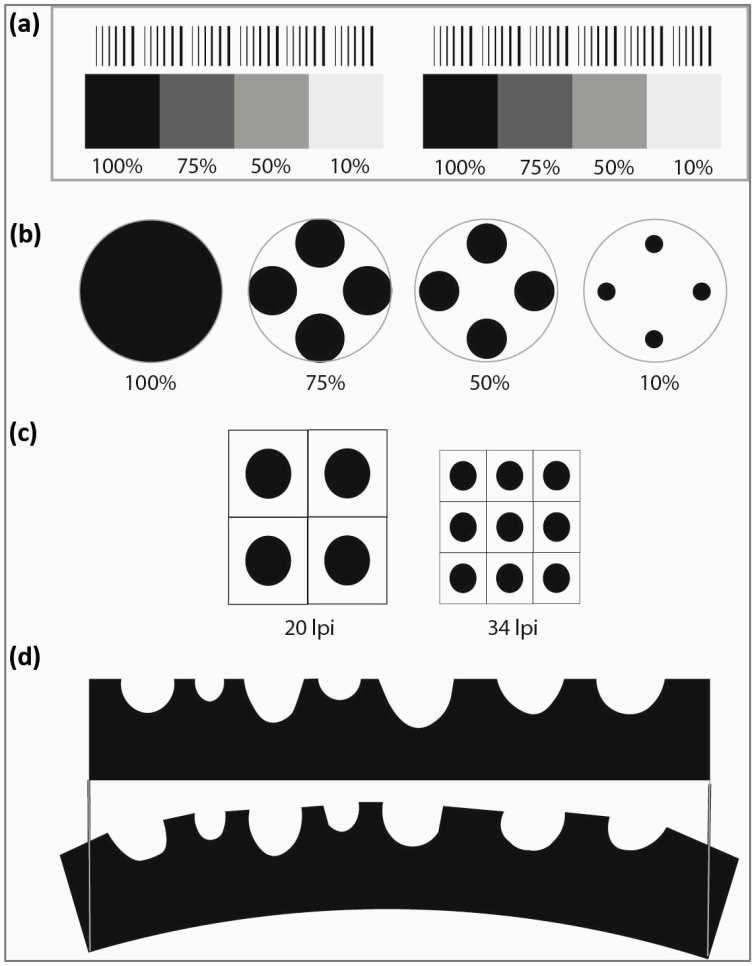


Figure 1. The printing plate design: (**a**) the distribution of the elements on the test plate, (**b**) the size of the raster points depending on the degree of surface coverage, (**c**) the comparison of the raster point sizes based on the linearity of the raster, and (**d**) the elongation of the drawing on the printing plate due to mounting on the plate cylinder.

In flexographic printing, there is an excessive enlargement of raster points in the highlights on the print due to the pressure applied during the printing process. Also, there is an elongation of the image elements on the printing plate depending on the circumference of the printing cylinder because of the mounting of the flat form on the cylinder surface. To eliminate these changes on the print, their formation should be considered during the manufacturing of the printing plate, and the drawing dimensions should be adjusted accordingly. Therefore, in order to make a CAD model in Autodesk Inventor (Figure 2), a

number of calculations were performed, as follows: percentage shortening of the negative in the printing direction (Figure 1d), radii of single raster points (Figure 1c) for two different printing plate lines, and radii of single raster points in the printing direction (shortened), for two different printing plate lines.

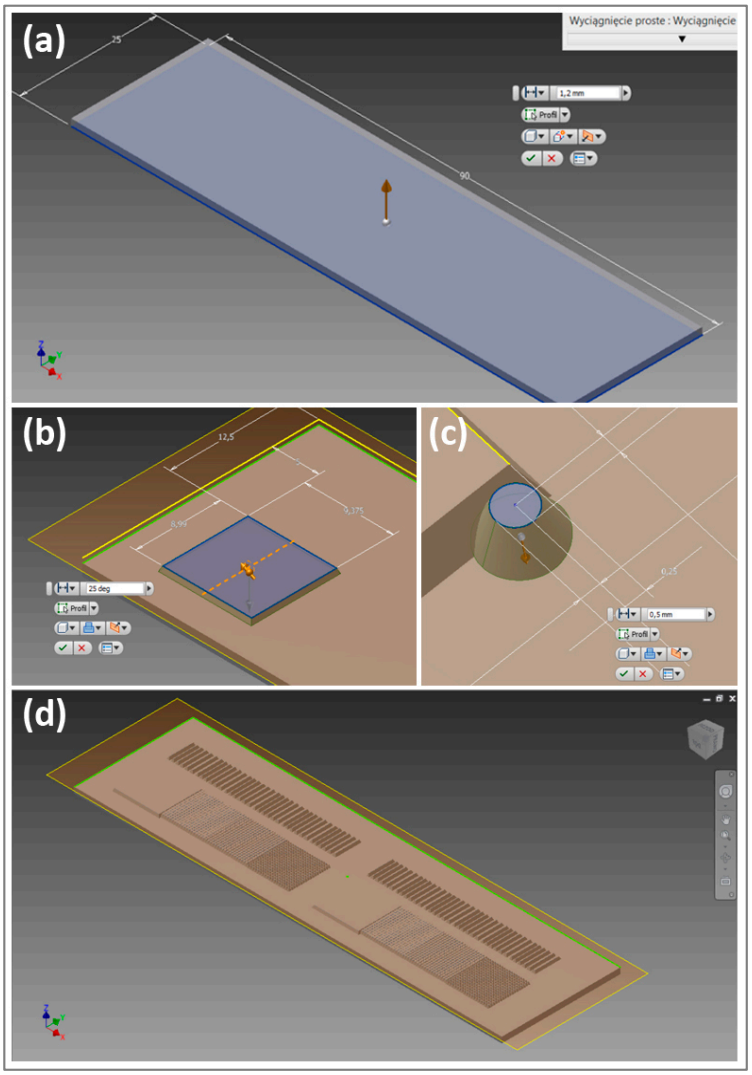


Figure 2. The design steps for the printing plate (**a**) the creation of a primer layer of 90 mm × 25 mm × 1.2 mm, similar to the pre-exposure process in conventional photopolymer plates, (**b**) the creation of a solid area on a test plate with a height of 0.5 mm and an inclination of 65° with respect to the base layer, (**c**) the preparation of a single raster point with dimensions taking into account the elongation in printing, which was then duplicated the appropriate number of times using a rectangular array operation to create a raster field of 10 mm × 10 mm, and (**d**) a finished design of a 3D-printing form with a linearity of 20 lpc.

The percentage shortening was calculated from Equation (1) [37],

$$SN = \frac{2\pi g}{L} \cdot 100\% \quad (1)$$

where the following variables are presented:

SN—shortening of the negative,
g—thickness of the printing form without substrate,
L—length of the printed image at one revolution of the printing cylinder.
The results of the calculations are shown in Table 1.

Table 1. Calculation of percentage shortening in printing direction.

Parameter	g [mm]	L [mm]	SN [%]
Value	1.7	260	4.11

The next step in the calculation was to calculate the radii needed for the raster fields of the test plate. The calculations were carried out for two values of printing plate rulings as follows: 20 lpc (lines per centimeter) and 34 lpc, matched to the raster cylinder rulings.

The results of the calculations are summarized in Table 2. The calculations were made as follows:

- the area of a single point was calculated, as a percentage of the area of a square with a side length of a fixed raster,
- the radius of the circle of a single point was calculated, using the area of the point,
- the shortened radius of the raster point was calculated (the radius of the raster point shortened by the percentage of the negative shortening).

Table 2. Raster point size calculations for 3D-printed flexographic plates.

Percentage Coverage [%]	Point Area [mm^2]	Single Point Radius [mm]	Raster Point Radius in Printing Direction [mm]
Test plate with 20 lpc linearity			
10	0.0250	0.0892	0.0855
50	0.1250	0.1995	0.1913
75	0.1875	0.2443	0.2343
Test plate with 34 lpc linearity			
10	0.0087	0.0525	0.0503
50	0.0433	0.1173	0.1125
75	0.0649	0.1437	0.1378

2.2. Printing Plates

The printing plates for the study were created using both PolyJet additive manufacturing technology and the traditional photopolymer technology typically used in the industry for producing flexographic plates. Figure 3 illustrates a comparison of the two methods of making printing plates.

The PolyJet test plates were produced on an Objet Connex350 machine (Stratasys, Tucson, AZ, USA) using TangoBlackPlus FLX9870-DM (Stratasys, Tucson, AZ, USA) photoresin. The resin has the following properties: hardness 68–72 Sh A, tensile strength 3.5–5.0 MPa, elongation at break 65–80%, and tensile tear resistance 15.5–17.5 Kg/cm. The plates (Figure 4a) were printed by RapidPro Company (Wrocław, Poland) based on the provided files containing digital models of the plates (Figure 2). Printing was done in high-quality modes and the layer height was 0.016 mm. The support material was removed using pressurized water at the post-processing stage.

The test printing plate was 90 mm wide and symmetrically divided into two zones of different linearity—it consists of two identical tests with a 6 mm notch between them. This notch is due to the design of the raster cylinder of the RK Print Flexiproof (RK Print Coat Instruments Ltd., Royston, UK) used for printing. The thickness of the printing plate was 1.7 mm, and the depth of the relief was 0.5 mm. Additionally, 10 samples of size 20 mm × 10 mm × 1.7 mm were printed for surface tension and chemical resistance tests of the test printing plate.

A 1.7-mm-thick photopolymer conventional plate nyloflex® FAH (BASF SE, Warsaw, Poland) (Figure 4b), prepared by Chespa (Chorula, Poland), was used for the comparative study. The conventional plate consisted of 6 tests with different screen rulings.

Further characteristics of the printing plates are presented in Table 3.

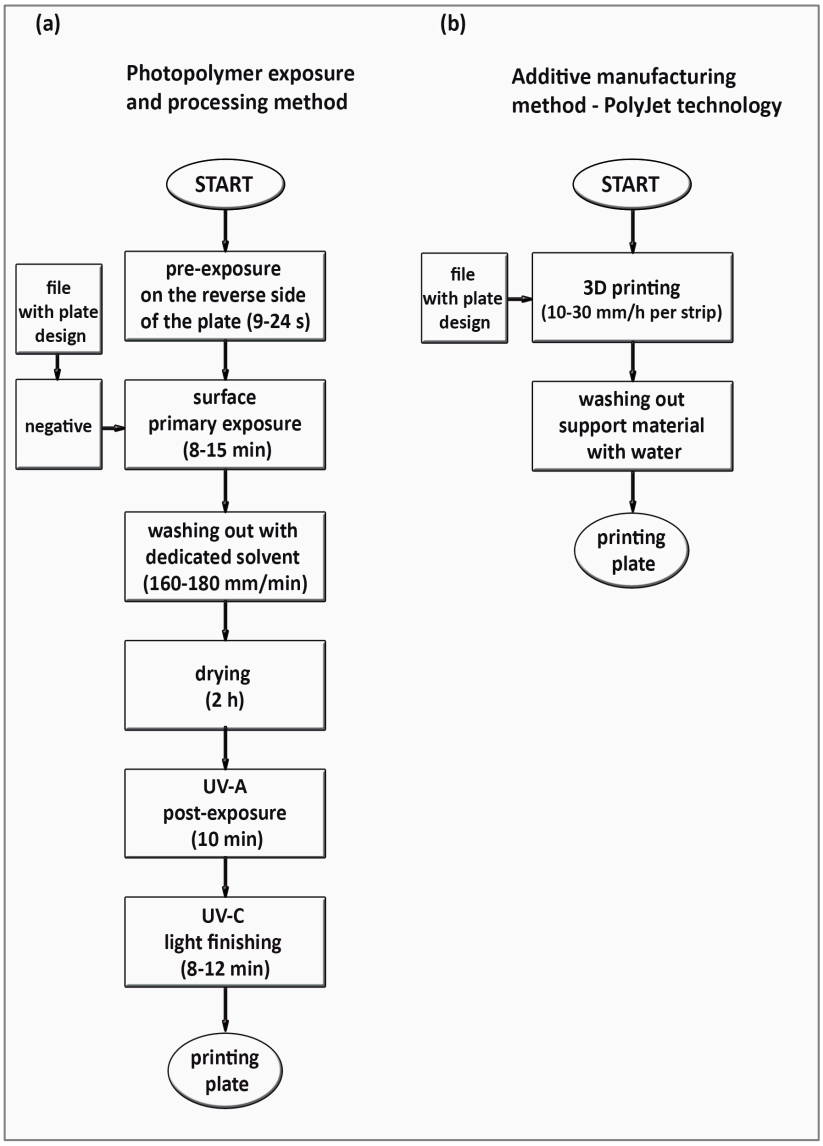


Figure 3. Schemes for making flexographic printing plates (**a**) traditional photopolymer, and (**b**) 3D-printed using PolyJet technology.

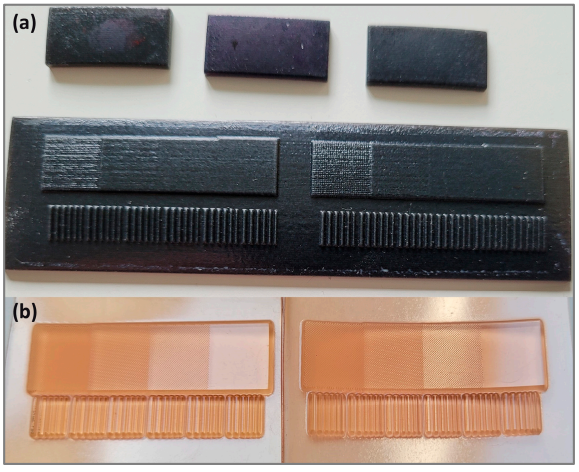


Figure 4. Photos of printing plates: (**a**) 3D-printed with linearity of 34 lpi and sample for chemical resistance testing and (**b**) conventional photopolymer with linearity of 42 lpi.

Table 3. Characteristics of printing plates.

Designation of Plate	F1	F2	F3	F4	F5
Technology of plate production	AM—PolyJet technology	AM—PolyJet technology	Photopolymer exposure and processing	Photopolymer exposure and processing	Photopolymer exposure and processing
Material	resin TangoBlack Plus	resin TangoBlack Plus	photopolymer	photopolymer	photopolymer
Color	black	black	red	red	red
Thickness [mm]	1.7	1.7	1.7	1.7	1.7
Thickness of relief [mm]	0.5	0.5	0.7	0.7	0.7
Screen ruling [lpc]	34	20	48	42	38

2.3. Testing of Printing Plates

In order to check the properties of the fabricated printing plates, chemical resistance and contact angle measurements were acquired.

The chemical resistance test was carried out by swelling based on PN-EN ISO 175:2010 [38]. Solvents widely used in the printing process and flexographic inks, namely distilled water, ethyl acetate, ethyl alcohol, acetone, isopropyl alcohol, propyl alcohol, a mixture of ethyl acetate and ethanol (chesol), water-based flexographic ink, solvent-based flexographic ink, and UV flexographic ink, were selected for the study. A 3D-printed plate sample and a conventional plate sample with dimensions 10 mm × 20 mm × 1.7 mm were used. Before starting the test, the width, length, thickness of the samples were measured using a caliper. The samples were then placed in beakers filled with either solvent or printing ink. Then, after 1, 2, or 4 h respectively, the samples were removed, dried with blotting paper, and the same dimensions were measured. Chemical resistance was determined as the percentage increase in sample volume calculated based on the change in sample dimensions. The volume value of the samples was calculated by multiplying the linear dimensions of the samples by themselves. The increment was calculated from Equation (2),

$$x_n = \frac{x - x_0}{x_0} * 100 \quad (2)$$

where the following variables are presented:

x_n—percentage increase,

x—value of volume at a given time,

x_0—value of volume before immersion of samples.

Surface contact angle measurements of both conventional and 3D-printed plates were carried out on a DSA30E (Krüss, Hamburg, Germany) using distilled water and diiodomethane 99% CH_2I_2 (Sigma-Aldrich, Taufkirchen, Germany). The Tangent method was used for the study. Drops of the substance with a constant volume of about 4 mL were applied to the surface of the printing plates and the contact angles were measured 15 s after the liquid drop was applied. The tests were carried out in constant environmental conditions and temperature 23 ± 1 °C. The results presented are the arithmetic averages of 5 measurements for each of the plates and measuring liquids. The determined values of the contact angle were used to calculate the values of the surface free energy of printing plates and their polar and dispersion components. The Owens–Wendt method [39] was used for the calculations.

2.4. Materials Used during Printing

The prints were made using water-based flexographic ink. The ink consisted of two components from the Hydro-X product family (Hubergroup Poland, Warsaw, Poland): a binder and a magenta base. The ingredients used were combined in a 1:1 ratio, and a light

purple color was obtained. The viscosity of the ink was set at 22 ± 1 s when measured with a Ø4 mm Ford cup (BYK Gardner, Germany), at an ambient temperature of 20 ± 0.5 °C.

Six different paper substrates were used in the study, which are characterized in Table 4.

Table 4. Characteristics of printing substrates used for flexographic printing.

Label	Type of Paper	Trade Name of Paper	Weight [g/m^2]
P1	coated	Test paper RK Print	-
P2	uncoated	International Paper Ballet Universal	80
P3	coated	Color Copy Cottage	250
P4	uncoated	Offset paper Igepa	90
P5	coated	ProfiSilk	300–350
P6	label, coated	Fasson MC Primecoat	82

2.5. Making Prints

To check the reproduction of the print, test prints were made on the FlexiProof 100 (RK Print Coat Instruments Ltd., Royston, UK). Prints were made on 6 paper substrates. In order to minimize measurement errors, 10 prints were made on each material. Prints were made using 2 3D-printed test plates and 3 conventional plates for one raster cylinder. A total of 10 usages were included in the print, each with different parameters (see Figure 5).

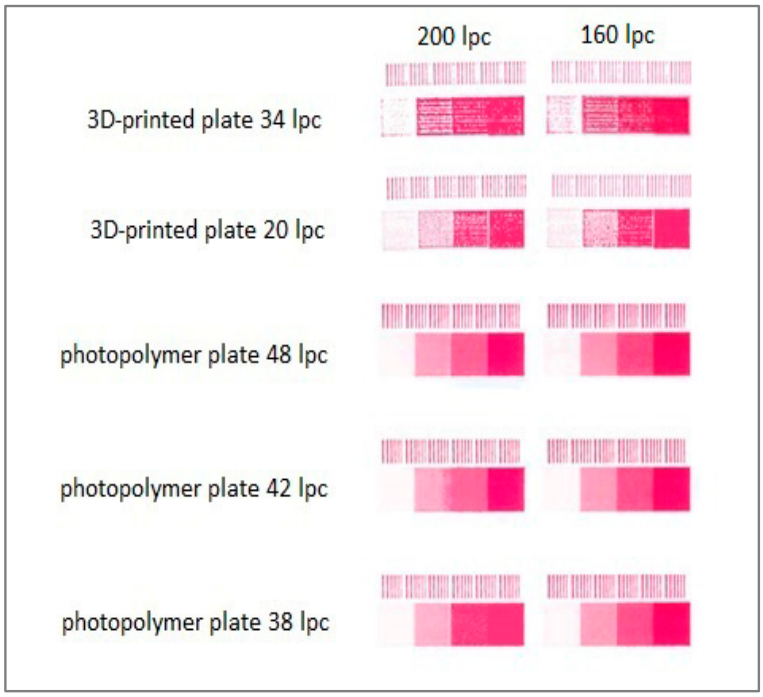


Figure 5. The image of a sample print with a description of the various reproduced elements arranged on it.

The prints were made at a speed of 60 m/min. The pressure between the plate cylinder and the raster cylinder was constant at 98 units. The pressure between the plate cylinder and the pressure cylinder was set individually for the substrates as follows: 45 units for uncoated substrates 2 and 4, 15 units for coated substrates 1and 6, and 10 units for coated substrates 3 and 5. These settings are those of the RK Print FlexiProof device, calculated from thickness of printing substrate, which define the correct printing pressure the so called kiss print [37,40].

A raster cylinder FLX100.02, numbered 66473 (RK Print Coat Instruments Ltd., Royston, UK), was used for printing. This ceramic anilox is symmetrically divided into two

engraved zones with line rulings of 200 lpc and 160 lpc. The raster angle for both rulings was 60°. The nominal capacity of the inkwells was 5 cm^3/m^2 and 6 cm^3/m^2.

Soft mounting tape (tesa, Hamburg, Germany), 0.5 mm thick, was used to mount the printing forms on the plate cylinder.

2.6. Print Quality Evaluation

The prints were evaluated for quality using a Gretag Spectroeye device (GretagMacbeth/X-Rite, Neu-Isenburg, Germany) to conduct densitometric and spectrophotometric measurements. The measurements were carried out under the following conditions: D50 illumination type, normal observer 2°, polarizing filter, and white standard—absolute and paper for color coordinate measurements and densitometric measurements, respectively. The color coordinates L^*, a^*, b^*, the optical density of solid fields, and the degree of percentage coverage of raster fields for 10 prints on each printing substrate were measured. The results presented are the arithmetic means.

2.7. Statistical Analysis

Statistical analysis was performed using the Excel data analysis toolkit (Office 365, Microsoft, Redmond, WA, USA). ANOVA and Tukey-Kramer post-hoc tests were employed to analyze the data. A significance level greater than 95% ($p < 0.05$) was considered indicative of significant differences.

3. Results and Discussions

3.1. Quality Analysis of Printing Plates

The results of the contact angle measurements with water and diiodomethane are summarized in Table 5. Based on these measurements, the values of surface free energy and its polar and dispersive components for the printing forms were determined using the Owens–Wendt method [39].

Table 5. Results of measurements of contact angles of printing plates and SFE values determined from them.

Printing Plate	Made with PolyJet Technology	Conventional
Water contact angle [°]	74.9 ± 1.8	75.4 ± 2.3
Diiodomethane contact angle [°]	45.5 ± 1.2	33.9 ± 1.4
SFE γ_L [mJ/m^2]	41.5	45.9
Polar SFE $\gamma_L{}^p$ [mJ/m^2]	4.8	3.4
Dispersive SFE $\gamma_L{}^d$ [mJ/m^2]	36.7	42.5

Both materials tested showed a similar wettability with water. However, the printing plates made conventionally show a higher wettability with diiodomethane than those made with 3D printing. This resulted in a higher SFE value and indicates better wettability. Moreover, this may have a direct impact on printing, or more specifically, on ink transfer through the printing plates [40]. When making prints, this may translate into the thickness of the ink layer on the print, which can be verified by measuring the optical densities of solid areas. Nonetheless, the obtained SFE and polar component values (Table 4) for the 3D-printed and conventional plates are not different enough to translate significantly into printability [19]. Flexographic inks should wet both conventional and 3D-printed plates and properly transfer ink to the substrate. As demonstrated by the study of the shape changes of the printing point, this even slightly lower SFE value of 3D-printed plates can lead to more homogeneous ink transfer from the plate to substrate [40].

Table 6 presents the results of the chemical resistance of the printing plates. The measurements were conducted for the 3D-printed plates and conventional plates. The table presents the percentage increase in the volume of the printing plate samples after being treated with solvents for specified times (1, 2, or 4 h), based on the measured values of the width, length, and thickness of the samples.

Table 6. Percentage increase in volume of samples.

Solvent	3D-Printed Plate			Conventional Photopolymer Plate		
	After 1 h	After 2 h	After 4 h	After 1 h	After 2 h	After 4 h
Water	2.79	0.55	1.96	1.52	0.45	1.21
Acetate	73.03	111.87	141.05	34.57	50.25	63.15
Ethanol	21.98	30.54	42.35	1.84	0.90	1.97
Acetone	89.10	Unk.	Unk.	12.43	15.80	21.11
Isopropanol	14.70	21.32	30.20	3.61	3.74	4.08
Npropanol	15.26	27.59	38.45	5.85	5.93	6.44
Chesol	22.02	31.48	48.69	1.21	9.49	8.71
Water-based ink	0.99	1.14	0.29	0.48	1.46	0.89
Solvent-based ink	23.07	38.93	56.69	7.28	6.86	6.09
UV ink	0.17	1.49	1.94	0.53	1.78	2.38

Unk.—means the inability to measure the sample due to damage.

The designation Unk. indicates the inability to measure a parameter. This was caused by damage to the sample—tearing or crushing that made the measurement impossible.

When analyzing the collected data, it is clear that the plates made using 3D printing do not exhibit adequate chemical resistance. The conventional plates showed less swelling regardless of the solvent used, although both tested materials demonstrated a low resistance to acetone and ethyl acetate. The 3D-printed plate treated with acetone was damaged after 2 h, preventing the measurement of the sample length, and the surface of the samples exhibited fractures. Conversely, after 4 h, the samples treated with ethyl acetate showed an increased brittleness, and their surfaces, similar to those immersed in acetone, were also fractured.

However, it should be noted that the 3D-printed samples tested behaved correctly in undiluted water-based and UV inks—they showed a small percentage increase in volume, like the values obtained for the conventional plates. The swelling in distilled water was also negligible.

Considering that 3D-printed samples exposed to more aggressive solvents exhibit a significant volume gain or even deteriorate, this disqualifies using TangoBlack Plus resin 3D-printed test plates for printing with solvent-based inks. In conclusion, the use of such a printing plate is unfortunately limited—they can be used when printing with water-based inks or UV inks. Special attention should be paid to the solvent used to wash the plate between and after printing to ensure it does not negatively affect the printing plate.

3.2. Evaluation of the Quality of Prints Made with Conventional Plates and Printed with PolyJet Technology

The evaluation of the quality of the prints included an analysis of the optical density (D) values of the solid fields, the L^*, a^*, b^* color coordinates, and the changes in the coverage of the raster fields (tone value changes). The effect of the type of flexographic printing plate, as well as the printing substrate and anilox ruling on the optical density values are shown in Figure 6.

The ANOVA test results for the optical density values ($F(59, 540) = 1.346$, $p = 0$) indicate significant differences between the group averages. The magnitude of the differences between the obtained values is significantly influenced by the raster cylinder ruling ($F(29, 270) = 1.510$, $p = 4.1 \times 10^{-196}$ and $F(29, 270) = 1.510$, $p = 3.3 \times 10^{-186}$ for L200 and L160, respectively). The prints with a 160 lpc cylinder ruling showed higher D values due to the higher ink capacity of their inkwells, resulting in more ink being transferred to the printing substrates.

Moreover, the conducted analysis revealed a significant influence of the type of flexographic printing plate on the obtained optical density results (Table 7). No significant differences were observed between the prints made using 3D-printed plates F1 and F2 regardless of the substrate and ruling type. Similarly, the prints made using the conventional

plates (F3, F4, and F5) showed no significant differences in their optical densities, except for a few cases: F3/F4 on the P1 substrate, and F3/F4 and F3/F5 on the P3 substrate, for prints made with L160 cylinder.

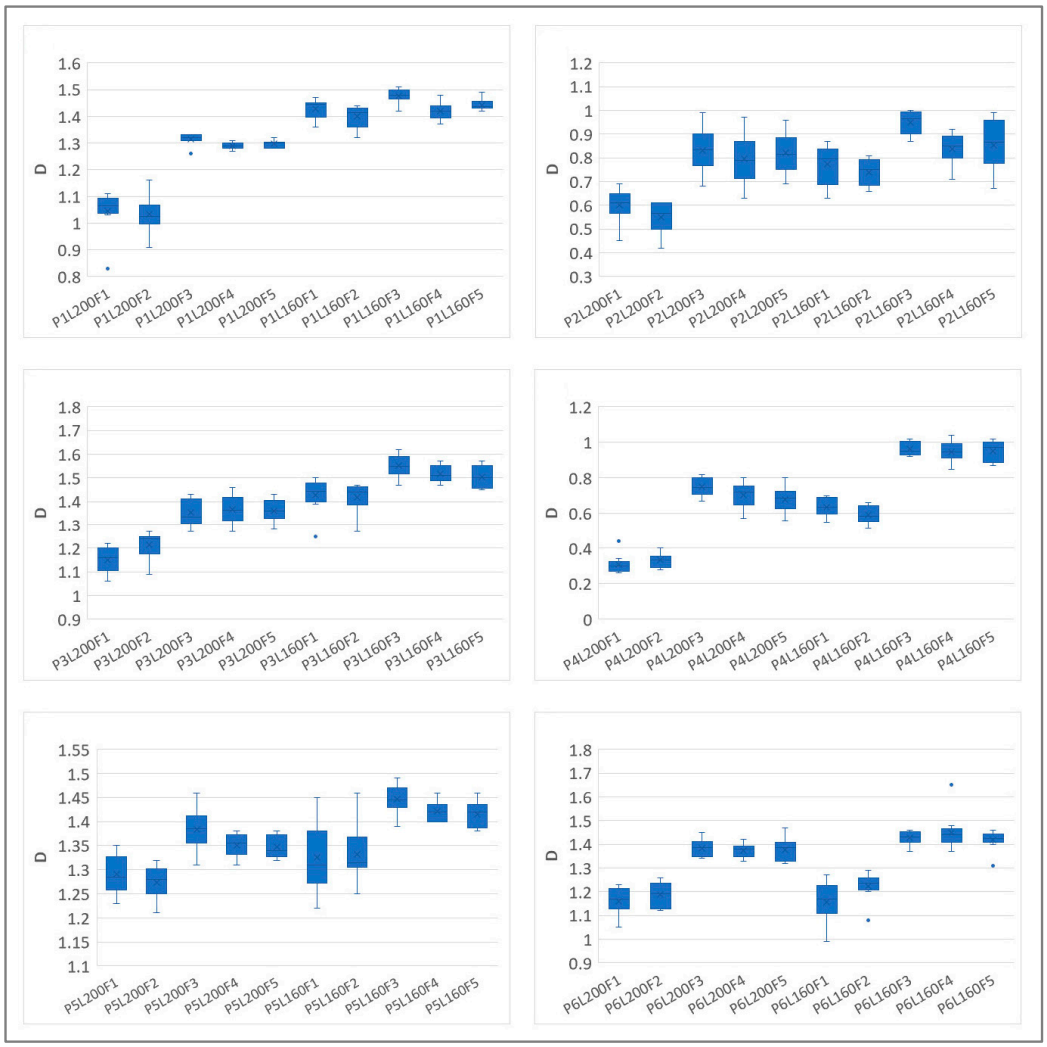


Figure 6. Optical density values of prints made with different printing plates (F1–F5), various raster cylinder rulings (L160 and L200), and multiple printing substrates (P1–P6).

Table 7. ANOVA test results for optical density values for different types of printing plates.

Printing Substrate	Raster Cylinder	
	200 lpc	**160 lpc**
P1	$F(4, 45) = 2.579$, $p = 7.67 \times 10^{-21}$	$F(4, 45) = 2.579$, $p = 3.28 \times 10^{-5}$
P2	$F(4, 45) = 2.579$, $p = 6.76 \times 10^{-11}$	$F(4, 45) = 2.579$, $p = 1.94 \times 10^{-6}$
P3	$F(4, 45) = 2.579$, $p = 2.17 \times 10^{-12}$	$F(4, 45) = 2.579$, $p = 1.60 \times 10^{-6}$
P4	$F(4, 45) = 2.579$, $p = 1.03 \times 10^{-24}$	$F(4, 45) = 2.579$, $p = 8.02 \times 10^{-25}$
P5	$F(4, 45) = 2.579$, $p = 8.58 \times 10^{-9}$	$F(4, 45) = 2.579$, $p = 1.37 \times 10^{-7}$
P6	$F(4, 45) = 2.579$, $p = 1.01 \times 10^{-16}$	$F(4, 45) = 2.579$, $p = 4.20 \times 10^{-15}$

On the other hand, the prints made with the 3D-printed flexographic plates exhibited significant differences in D values compared to those made with the conventional plates. Only the prints obtained using a 3D-printed plate with a 34 lpc (F1) ruler and a 160 lpc raster cylinder did not differ significantly from those obtained using the same raster cylinder and

the conventional printing plates F4 and F5. Furthermore, the solid areas printed with the 3D-printed flexographic plates had a lower optical density compared to the prints from the conventional plates. The differences in optical densities were greater for the measurements of the prints obtained using a 200 lpc raster cylinder ruling. For the coated substrates, they range from 0.10 to 0.30, while for the uncoated substrates, the difference is greater, ranging from 0.2 to 0.4 depending on the substrate.

The L^*, a^*, b^* color coordinate measurements indicate that the reproduced colors vary significantly among the different prints ($0.1 \leq \Delta E \leq 58.4$). Notable variations in lightness (L^*) values were confirmed by the ANOVA test results ($F(59, 540) = 1.346$, $p = 0$). The prints made with the 3D-printed flexographic plates are lighter and less saturated compared to those obtained with the conventional plates (Figure 7). Moreover, similar to the D value, both the printing substrate and the raster cylinder ruling used significantly affect the results. Consistent with the optical density findings, the results of the measurements for the prints obtained using a raster cylinder ruling of 200 lpc are lighter than those obtained with a ruling of 160 lpc, which is directly related to the inkwell capacity of the cylinders—cylinders with smaller linings have larger inkwells, allowing for greater ink transfer. Considering the printing substrates, the uncoated substrates (P3 and P5) yielded significantly higher L^* values, i.e., lighter prints, compared to those made on coated substrates. This difference can be attributed to the variations in substrate absorbency. Additionally, the use of 3D-printed flexographic plates led to even higher L^* values (differences of up to 15–17%). These variations in lightness significantly impact the resulting color.

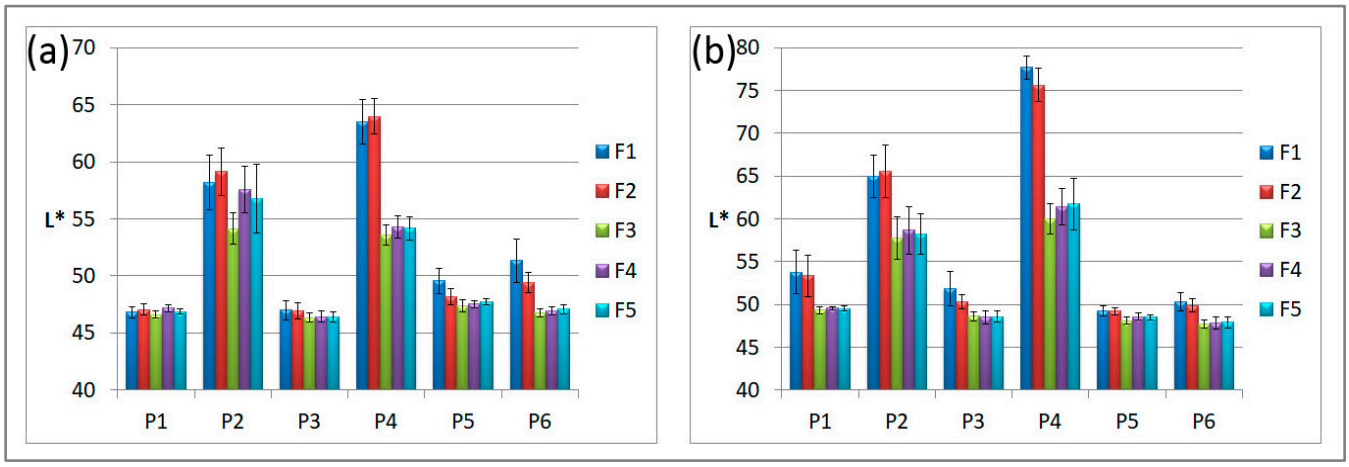


Figure 7. Average lightness of prints obtained on multiple substrates (P1–P6) using different printing plates (F1–F5) and various raster cylinder rulings of (**a**) 160 lpc and (**b**) 200 lpc.

In analyzing the measurements of percentage coverage, it is evident that full consistency cannot be achieved on any of the considered substrates, regardless of the raster cylinder used (Figure 8). The highest level of agreement in the measurements was observed for the coated substrates at fields with 75% coverage. The 3D-printed flexographic plates of 34 lpc (F1) correlated with the conventional plates labeled 4–5, which correspond to 42 lpc and 38 lpc, respectively. The measurements of the degree of percentage coverage for a 3D-printed flexographic plate of 20 lpc (F2) for fields of 75% are lower than the averages for the conventional plates. The percent coverage rate for the uncoated substrates has a value lower than the conventional plates for both 3D-printed flexographic plates and raster cylinders. Regarding the percentage coverages of 50% and 10%, we cannot speak of the correct reproduction. Some correlation of the measurement results was noticeable, but this is insufficient due to the lack of visual mapping. Unfortunately, the 3D-printing technology and the resin used did not allow us to obtain the correct raster points on the flexographic plates and reproduce them in the printing process.

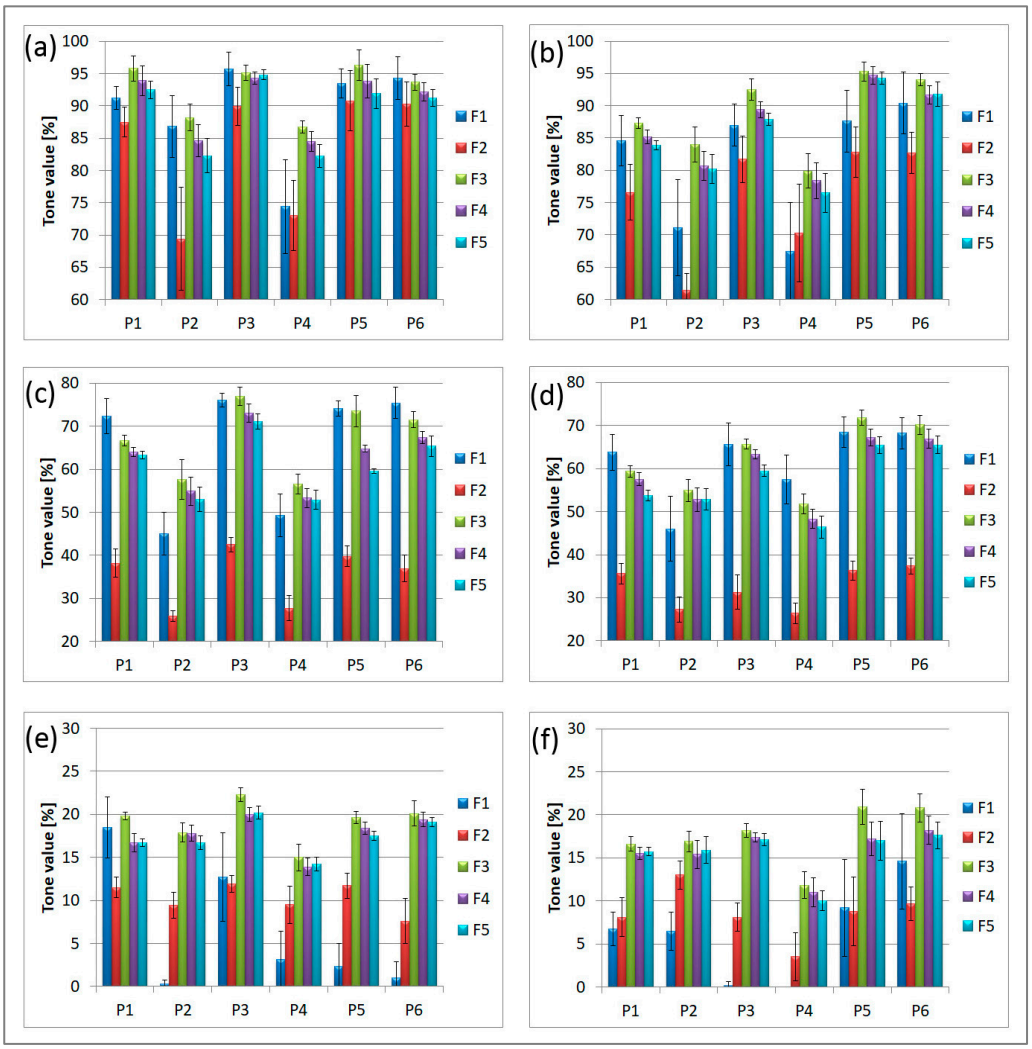


Figure 8. Average measured values of percentage coverage of raster fields of prints made on different substrates (P1–P6) using multiple printing plates (F1–F5) with various raster cylinder rulings of (**a**) 160 lpc field 75%, (**b**) 200 lpc field 75%, (**c**) 160 lpc field 50%, (**d**) 200 lpc field 50%, (**e**) 160 lpc field 10%, and (**f**) 200 lpc field 10%.

3.3. Summary of the Results and Future Research Directions

This comparative study revealed that 3D-printed plates made using PolyJet technology exhibit different physical properties compared to conventional plates. The resin used in this study demonstrates low resistance to most solvents commonly employed in printing houses, limiting its application to water-based and UV printing inks and unfortunately excludes solvent-based inks, which constitute the majority of flexographic printing inks. Given the variety of resins available in the market, exploring other rubber-like materials in future research would be beneficial.

The plates prepared using PolyJet technology enable printing with water-based inks, however, the quality of these prints is relatively low and does not meet current expectations for flexographic printing. A satisfactory reproduction quality is only achievable for solid printed areas (apla) and lines, while significant challenges arise with the reproduction of raster fields. It has been observed that a correct raster grid cannot be obtained with the PolyJet technology and the material used. To address this issue, it may be worthwhile to explore the possibility of creating a 3D-printed plate using a different resin. Despite the high precision of the PolyJet technology, it would be worthwhile to check the possibility of

reproducing raster points using other AM technologies or to optimize the parameters of the PolyJet printing process.

In summary, the challenges associated with the reproduction of the raster points may stem from the inadequate manufacturing quality of the raster structures on the printing plate, the hardness of the 3D-printed plate due to the properties of the resin, which affects ink transfer, or the design of the printing form itself. Further research seems valuable and would allow us to explore the use of PolyJet technology to produce flexographic plates using different parameters of the 3D-printing process and alternative resins. Additionally, it may be worthwhile to consider the design of new printing plates with modified raster dot shapes, such as a different cone angle, vertex shape, or relief depth. However, material type appears to be a crucial factor, as the 3D-printed plates transferred less ink to the printing substrate, resulting in test prints characterized by a lower optical density and higher lightness. Furthermore, the quality of the prints is significantly affected by the print substrate; better results were obtained on coated substrates compared to uncoated ones. Given the widespread use of films in flexographic printing, it would be worthwhile to incorporate such a substrate in future studies.

4. Conclusions

PolyJet technology enables the production of flexible printing plates suitable for flexographic printing of lines and solid areas with water-based ink. However, the high-quality printing of raster fields was not achieved. Moreover, the plates printed with TangoBlack Plus resin appear to be suitable for printing with UV inks due to their high resistance, but they are not resistant to the solvents used in solvent-based inks.

Despite the small differences in SFE values between the 3D-printed and traditional photopolymer plates (42 and 46 mJ/m^2, respectively), significant differences in ink transfer to the print substrate were observed (D values of areas were in the range of 0.51–1.5 for L160 and 0.26–1.35 for L200, and 0.67–1.62 for L160 and 0.56–1.46 for L200, respectively). However, these differences in quality were significantly related to the type of substrate used. A significantly better print quality was achieved on coated substrates compared to uncoated substrates (the optical density for uncoated papers was $\leq$1) with the prints made using the 3D-printed plates having a D value that was 10–20% lower than those made with the photopolymer plates. Furthermore, the reproduction of the raster fields was not satisfactory for most of the prints made with the 3D-printed plates, with only the raster fields with 75% coverage on the coated papers being reproduced with a high quality.

Further research into the use of AM and PolyJet technology in the production of flexographic printing plates is essential.

Author Contributions: Conceptualization and methodology, J.I.-P. and A.L.; validation, J.I.-P.; formal analysis, J.I.-P.; investigation, A.L.; resources, J.I.-P. and A.L.; writing—original draft preparation, J.I.-P.; writing—review and editing, J.I.-P.; visualization, J.I.-P.; supervision, J.I.-P. All authors have read and agreed to the published version of the manuscript.

Funding: This research received no external funding.

Institutional Review Board Statement: Not applicable.

Informed Consent Statement: Not applicable.

Data Availability Statement: The original contributions presented in the study are included in the article, further inquiries can be directed to the corresponding author.

Conflicts of Interest: The authors declare no conflicts of interest.

References

1. Mordorintelligence. Flexographic Printing Industry—Size, Share & Industry Analysis. Available online: https://www.mordorintelligence.com/industry-reports/flexographic-printing-market (accessed on 1 February 2024).
2. Smithers. The Future of Flexographic Printing to 2027. Market Reports & Research. Available online: https://www.smithers.com/services/market-reports/printing/the-future-of-flexographic-printing-to-2027 (accessed on 1 February 2024).

3. Smithers. The Future of Print to 2030. Market Reports and Data. Available online: https://www.smithers.com/services/market-reports/printing/the-future-of-print-to-2030 (accessed on 1 February 2024).
4. Izdebska, J. Ch 11—Flexographic Printing. In *Printing on Polymers*; Izdebska, J., Thomas, S., Eds.; William Andrew Publishing: Waltham, MA, USA, 2016; pp. 179–197. [CrossRef]
5. Kipphan, H. *Handbook of Print Media: Technologies and Production Methods*; Springer: New York, NY, USA, 2001.
6. Grandviewresearch. Commercial Printing Market Size, Share & Trends Report. 2030. Available online: https://www.grandviewresearch.com/industry-analysis/commercial-printing-market (accessed on 1 February 2024).
7. Zenkin, M.; Makatora, D.; Ivanko, A.; Makatora, A. The analysis of printing equipment manufacturing. *AD ALTA-J. Interdiscipinary Res.* **2022**, 69–72.
8. Ejsmont, K.; Lipiak, J. The Model of Assessment for Flexographic Printing Technology. In *Proceedings of the 8th International Conference on Engineering, Project, and Product Management (EPPM 2017), 19–21 September 2017, Amman, Jordan, Lecture Notes in Mechanical Engineering*; Şahin, S., Ed.; Springer: Cham, Switzerland, 2018. [CrossRef]
9. Mavri, M.; Fronimaki, E.; Kadrefi, A. Survey analysis for the adoption of 3D printing technology: Consumers' perspective. *J. Sci. Technol. Policy Manag.* **2023**, *14*, 353–385. [CrossRef]
10. *ISO/ASTM52900:2021*; Additive Manufacturing—General Principles—Fundamentals and Vocabulary. ISO: Geneva, Switzerland, 2021. Available online: https://www.iso.org/obp/ui/#iso:std:iso-astm:52900:ed-2:v1:en (accessed on 18 September 2024).
11. Izdebska-Podsiadły, J. (Ed.) Chapter 3—Classification of 3D printing methods. In *Plastics Design Library, Polymers for 3D Printing*; William Andrew Publishing: Cambridge, MA, USA, 2022; pp. 23–34. [CrossRef]
12. Park, S.; Shou, W.; Makatura, L.; Matusik, W.; Fu, K. 3D printing of polymer composites: Materials, processes, and applications. *Matter* **2022**, *5*, 43–76. [CrossRef]
13. Ali, M.H.; Batai, S.; Sarbassov, D. 3D printing: A critical review of current development and future prospects. *Rapid Prototyp. J.* **2019**, *25*, 1108–1126. [CrossRef]
14. Izdebska-Podsiadły, J. (Ed.) Chapter 4—Materials for 3D printing. In *Plastics Design Library, Polymers for 3D Printing*; William Andrew Publishing: Cambridge, MA, USA, 2022; pp. 35–49. [CrossRef]
15. Arefin, A.M.E.; Khatri, N.R.; Kulkarni, N.; Egan, P.F. Polymer 3D Printing Review: Materials, Process, and Design Strategies for Medical Applications. *Polymers* **2021**, *13*, 1499. [CrossRef] [PubMed]
16. Herzberger, J.; Sirrine, J.M.; Williams, C.B.; Long, T.E. Polymer Design for 3D Printing Elastomers: Recent Advances in Structure, Properties, and Printing. *Prog. Polym. Sci.* **2019**, *97*, 101144. [CrossRef]
17. Schniederjans, D.G. Adoption of 3D-printing technologies in manufacturing: A survey analysis. *Int. J. Prod. Econ.* **2017**, *183*, 287–298. [CrossRef]
18. Izdebska-Podsiadły, J. (Ed.) Chapter 5—Application of 3D printing. In *Plastics Design Library, Polymers for 3D Printing*; William Andrew Publishing: Cambridge, MA, USA, 2022; pp. 51–62. [CrossRef]
19. Liu, X.; Guthrie, J.T. A review of flexographic printing plate development. *Surf. Coat. Int. Part B Coat. Trans.* **2003**, *86*, 91–99. [CrossRef]
20. Johnson, J. Aspects of Flexographic Print Quality and Relationship to Some Printing Parameters. Ph.D. Thesis, Karlstad University, Karlstad, Sweden, 2008.
21. Shahrubudin, N.; Lee, T.C.; Ramlan, R. An Overview on 3D Printing Technology: Technological, Materials, and Applications. *Procedia Manuf.* **2019**, *35*, 1286–1296. [CrossRef]
22. Reza, K.M.; Reinicke, T. Effects of raster layup and printing speed on strength of 3D-printed structural components. *Procedia Struct.* **2020**, *28*, 720–725.
23. Bould, D.C.; Claypole, T.C.; Bohan, M.F.J.; Gethin, D.T. Deformation of Flexographic Printing Plates. In Proceedings of the 56th TAGA Technical Conference, TAGA, San Antonio, TX, USA, 20 April 2004; pp. 146–162.
24. Valdec, D.; Hajdek, K.; Vragović, L.; Geček, R. Determining the Print Quality Due to Deformation of the Halftone Dots in Flexography. *Appl. Sci.* **2021**, *11*, 10601. [CrossRef]
25. Das, S.H.; Ranganathan, R.; Murugan, N. Effect of build orientation on the strength and cost of PolyJet 3D printed parts. *Rapid Prototyp. J.* **2018**, *24*, 832–839. [CrossRef]
26. Piłczyńska, K. Chapter 8—Material jetting. In *Plastics Design Library, Polymers for 3D Printing*; Izdebska-Podsiadły, J., Ed.; William Andrew Publishing: Cambridge, MA, USA, 2022; pp. 91–103. [CrossRef]
27. Mayyas, M. Interpolation of tensile properties of polymer composite based on Polyjet 3D printing. *Prog. Addit. Manuf.* **2021**, *6*, 607–615. [CrossRef]
28. Ulu, F.; Tomar, R.P.S.; Mohan, R. Processing and mechanical behavior of rigid and flexible material composite systems formed via voxel digital design in polyjet additive manufacturing. *Rapid Prototyp. J.* **2021**, *27*, 617–626. [CrossRef]
29. Palanisamy, C.; Raman, R.; Dhanraj, P.K. Additive manufacturing: A review on mechanical properties of polyjet and FDM printed parts. *Polym. Bull.* **2022**, *79*, 7065–7116. [CrossRef]
30. Kechagias, J.; Stavropoulos, P.; Koutsomichalis, A.; Ntintakis, I.; Vaxevanidis, N. Dimensional Accuracy Optimization of Prototypes produced by PolyJet Direct 3D Printing Technology. *Adv. Eng. Mech. Mat.* **2014**, 61–65.
31. Maksud, M.I.; Nodin, M.N.; Yusof, M.S.; Hassan, S. Utilizing rapid prototyping 3D printer for fabricating flexographic PDMS printing plate. *ARPN J. Eng. Appl. Sci.* **2016**, *11*, 7728–7734.

32. Huang, B.; Shang, X.; Li, Y.; Wei, X.; Guo, C. Study of Printability of Hybrid Light Curable Material Used in 3D Printing—Product Flexographic Plate. In *Advanced Graphic Communications and Media Technologies. PPMT 2016*; Lecture Notes in Electrical Engineering; Zhao, P., Ouyang, Y., Xu, M., Yang, L., Ouyang, Y., Eds.; Springer: Singapore, 2017; Volume 417. [CrossRef]
33. Tsakos, D. Implementation of 3D Printing Technology in Flexographic Packaging Printing. Master's Thesis, Aalborg University, Aalborg East, Denmarks, 2018.
34. Zheng, L.; Kong, L.; Li, C. Feasibility Study of Flexographic Platemaking Based on SLA 3D Printing Technology. In *Advances in Graphic Communication, Printing and Packaging*; Lecture Notes in Electrical Engineering; Zhao, P., Ouyang, Y., Xu, M., Yang, L., Ren, Y., Eds.; Springer: Singapore, 2019; Volume 543. [CrossRef]
35. Hassan, S.; Yusof, M.S.; Embong, Z.; Ding, S.; Marwah, O.M.F. A study of printing plate mould development by using 3D printers for micro-flexographic printing process. *JAMT* **2020**, *14*, 25–36.
36. Zheng, L. Analysis of Factors Affecting Flexographic Plate-Making Technology Based on Surface Imaging Stereolithography. In *Advances in Graphic Communication, Printing and Packaging Technology and Materials*; Lecture Notes in Electrical Engineering; Zhao, P., Ye, Z., Xu, M., Yang, L., Zhang, L., Zhu, R., Eds.; Springer: Singapore, 2021; Volume 754. [CrossRef]
37. Czichon, H.; Czichon, M. *Fleksodruk. Formy Drukowe i Materiały (Flexo Printing. Printing Plates and Materials)*; OWPW: Warsaw, Poland, 2014.
38. *ISO 175:2010 Plastics*; Methods of Test for the Determination of the Effects of Immersion in Liquid Chemicals, 3rd ed. ISO: Geneva, Switzerland, 2010.
39. Owens, D.K.; Wendt, R.C. Estimation of the surface free energy of polymers. *J. Appl. Polym. Sci.* **1969**, *13*, 1741–1747. [CrossRef]
40. Valdec, D.; Miljkovic, P.; Čerepinko, D. The Impact of Top Dot Shapes of the Printing Plate on Dot Formation in Flexography. *Tech. Gaz.* **2018**, *25*, 596–602. [CrossRef]

Disclaimer/Publisher's Note: The statements, opinions and data contained in all publications are solely those of the individual author(s) and contributor(s) and not of MDPI and/or the editor(s). MDPI and/or the editor(s) disclaim responsibility for any injury to people or property resulting from any ideas, methods, instructions or products referred to in the content.